DOI: 10.25092/baunfbed.340553 *J. BAUN Inst. Sci. Technol., 19(2), 99-115, (2017)*

Theoretical studies of molecular structure, spectroscopic, electronic and NLO investigations of Oxamyl

Aslı EŞME[*]

Kocaeli University, Faculty of Education, Department of Mathematics and Science Education, 41380, Umuttepe, Kocaeli.

Geliş Tarihi (Recived Date): 24.05.2017
Kabul Tarihi (Accepted Date): 17.08.2017

Abstract

The optimized geometrical structures, harmonic vibrational wavenumbers, the highest occupied molecular orbital (HOMO) energies, the lowest unoccupied molecular orbital (LUMO) energies, the electronic properties (total energy, dipole moment, electronegativity, chemical hardness and softness), molecular surfaces, and nonlinear optical (NLO) parameters [mean polarizability <α>, the anisotropy of the polarizability ⟨Δα⟩, and the mean first-order hyperpolarizability <β >] of oxamyl [N,N-dimethyl-2-methylcarbamoyloxymino-2-(methylthio) acetamide] been investigated by the Hartree-Fock (HF) and Density Functional Theory (DFT) using B3LYP functional with 6-311++G(d,p) basis set.

Keywords: *N,N-dimethyl-2-methylcarbamoyloximino-2-(dimethylsulfanyl)acetamide, DFT, HF, VEDA, Nonlinear optical (NLO) parameters.*

Oksamil molekülünün moleküler yapısının, spektroskopik, elektronik ve NLO özelliklerinin teorik olarak incelenmesi

Özet

6-311++G(d,p) temel seti ile yoğunluk fonksiyonu teorisi (DFT/B3LYP) ve Hartree-Fock (HF) metodları kullanılarak geometrik parametreleri (bağ uzunlukları ve bağ açıları), harmonik titreşim dalga sayıları, en yüksek dolu moleküler orbital (HOMO) ve en düşük boş moleküler orbitallerin (LUMO) enerjileri, elektronik özellikleri (toplam enerji, dipol moment, elektronegativite, kimyasal sertlik ve yumuşaklık), moleküler yüzeyler, ve doğrusal olmayan optik (NLO) parametreleri [kutuplanabilirlik <α>,

[*] Aslı EŞME, asli.esme@kocaeli.edu.tr, http://orcid.org/0000-0002-8964-0631

yönelime bağlı kutuplanabilirlik ⟨Δα⟩, ve statik yüksek mertebe kutuplanabilirlik <β>] Gaussian 09W programı kullanılarak incelendi.

Anahtar kelimeler: *N,N-dimetil-2-methilkarbamoyloksimino-2-(dimetilsulfanil) asetamid, DFT, HF, VEDA, doğrusal olmayan optik (NLO) parametreleri***.**

1. Introduction

Carbamate-type pesticides are characterized by their broad spectrum toxicity, high solubility in water, and fast degradation of the active compound [1]. The use of large quantities of pesticides in agriculture practices is one of the main causes of soil pollution. Oxamyl (*N,N*-dimethyl-2-methylcarbamoyloximino-2-(dimethylsulfanyl) acetamide) is a carbamate compound used in a wide range of agricultural situations. It is systemic and active as an insecticide/nematicide which is extensively used in India for controlling the growth of nematodes in vegetables, bananas, pineapple, peanuts, cotton, soya beans, tobacco, potatoes, sugar beet, and other crops. In spite of its short half-life in soils, it may represent an environmental risk because of its high solubility in water and toxicity [2] to such an extent that it has been detected in ground waters of the Netherlands [3]. It possesses severe detrimental and toxicological effects on the prevailing flora and fauna of the particular ecosystem as well as in living beings. If it enters the biological cycle of the human, it inhibits the acetylcholinesterase by the rapid carbamylation of its active site [4, 5].

The oxamyl was synthesized and crystal structure is characterized with X-ray diffraction method by E. Kwon et al. [6]. Literature survey reveals that to the best of our knowledge no ab initio Hartree-Fock (HF) and Density Functional Theory (DFT) spectroscopic and harmonic vibrational frequency calculations of oxamyl have been reported up to the present. The objective of the present study was to provide a complete description of the molecular geometry, and the vibrational spectra of the studied molecule. Hence, we characterized the molecular structure, NLO analysis, vibrational frequencies, total energy, E_{HOMO} and E_{LUMO} energies, electronegativity (χ), global hardness (η), and global softness (σ), molecular electrostatic potential (MEP) maps, and the molecular surfaces of the molecule in the ground state and also calculated at the Hartree-Fock (HF) and Density Functional Theory (DFT) levels with the 6-311++G(d,p) basis set. Vibrational spectra of the studied molecule have been analyzed on the basis of calculated potential energy distribution (PED).

2. Computational procedure

The whole calculations of oxamyl were carried out by using Gaussian 09 Rev. A 11.4 [7] software package and obtained results were visualized by means of the Gauss View Rev. 5.0.9 [8] software. The molecular structure of the oxamyl in the ground state was optimized using Density Functional Theory (DFT) with the Becke-3-Lee–Yang–Parr (B3LYP) functional [9,10] level for the 6-311++G(d,p) basis set. Detailed assignments of vibrational modes were carried out based on percentage potential energy distribution (PED) analysis using the VEDA4 program written by Jamroz. [11]. At the optimized structures of the molecule no imaginary frequency modes were obtained, providing that a true minimum on the potential energy surface was found. The scale factors are used

to obtain the best agreement results between the calculated and experimental frequencies. The vibrational frequencies for the title compound are calculated with these methods and then wavenumbers in the ranges from 4000 to 1700 cm^{-1} and lower than 1700 cm^{-1} are scaled with 0.958 and 0.9067, and 0.983 and 0.958 in the DFT/B3LYP and HF levels, respectively [12]. Highest occupied molecular orbital (HOMO) and lowest unoccupied molecular orbital (LUMO) calculations were made at the same level of theory.

In the context of the HF theorem, the E_{HOMO} and E_{LUMO} is used to approximate the ionization potential (I) and electron affinity (A) given by Koopmans' theorem [13], respectively. Although no formal proof of this theorem exists within density functional theory (DFT), its validity is generally accepted. DFT has been to be successful in providing insights into the chemical reactivity, in terms of molecular parameters such as global hardness (η), global softness (σ) and electronegativity (χ).

I and A are related to

$$I = -E_{HOMO} \qquad A = -E_{LUMO} \tag{1}$$

The global hardness (η) is a measure the resistance of an atom to charge transfer [14] and it can calculated as

$$\eta = \left(\frac{\mathrm{I}-\mathrm{A}}{2}\right) = -\frac{1}{2}\left(\mathrm{E_{HOMO}} - \mathrm{E_{LUMO}}\right) \tag{2}$$

The global softness (σ) describes the capacity of an atom or a group of atoms to receive electrons [14] and is equal to reciprocal of global hardness.

$$\sigma = \frac{1}{\eta} = -\frac{2}{\left(\mathrm{E_{HOMO}} - \mathrm{E_{LUMO}}\right)} \tag{3}$$

Electronegativity (χ) is a measure of the power of an atom or a group of atoms to attract electrons towards itself [15] and can be calculated from HOMO-LUMO as

$$\chi = \left(\frac{\mathrm{I}+\mathrm{A}}{2}\right) = -\frac{1}{2}\left(\mathrm{E_{HOMO}} + \mathrm{E_{LUMO}}\right) \tag{4}$$

Polarizabilities were calculated at the same level of theory using the standard GAUSSIAN-09W keyword 'Polar' [16]. This keyword means that the polarizabilities were obtained analytically rather than by numerical differentiation.

The energy of an uncharged molecule under a weak, general electric field can be expressed by Buckingham type expansion [17-19]

$$E = E_0 - \mu_i F_i - (1/2)\alpha_{ij} F_i F_j - (1/6)\beta_{ijk} F_i F_j F_k - (1/24)\gamma_{ijkl} F_i F_j F_k F_l - \ldots\ldots \tag{5}$$

where E is the energy of a molecule under the electric field F, E_0 is the unperturbed energy of a free molecule, F_i is the vector component of the electric field in the i

direction, and μ_i , α_{ij} , β_{ijk} , γ_{ijkl} are the dipole moment, the mean polarizability, first-order hyperpolarizability, and second-order hyperpolarizability, respectively. Here, each subscript of *i*, *j*, *k*, and *l* denotes the indices of the Cartesian axes *x*, *y*, *z*, and a repeated subscript means a summation over the Cartesian indices *x*, *y*, *z*. The ground state dipole moment (μ), the mean polarizability ($<\alpha>$), the anisotropy of the polarizability ($<\Delta\alpha>$) and the mean first-order hyperpolarizability (β), using the x, y, z components they are defined as [20, 21]

$$\mu = \left(\mu_x^2 + \mu_y^2 + \mu_z^2\right)^{1/2} \tag{6}$$

$$\langle\alpha\rangle = \frac{\alpha_{xx} + \alpha_{yy} + \alpha_{zz}}{3} \tag{7}$$

$$\langle\Delta\alpha\rangle = \left[\frac{\left(\alpha_{xx} - \alpha_{yy}\right)^2 + \left(\alpha_{yy} - \alpha_{zz}\right)^2 + \left(\alpha_{zz} - \alpha_{xx}\right)^2 + 6\left(\alpha_{xy}^2 + \alpha_{xz}^2 + \alpha_{yz}^2\right)}{2}\right]^{1/2} \tag{8}$$

$$\beta = \sqrt{\left(\beta_{xxx} + \beta_{xyy} + \beta_{xzz}\right)^2 + \left(\beta_{yyy} + \beta_{yzz} + \beta_{yxx}\right)^2 + \left(\beta_{zzz} + \beta_{zxx} + \beta_{zyy}\right)^2}\,. \tag{9}$$

The mean polarizability and mean first-order hyperpolarizability tensors ($\alpha_{xx}, \alpha_{xy}, \alpha_{yy}, \alpha_{xz}, \alpha_{yz}, \alpha_{zz}$ and $\beta_{xxx}, \beta_{xxy}, \beta_{xyy}, \beta_{yyy}, \beta_{xxz}, \beta_{xyz}, \beta_{yyz}, \beta_{xzz}, \beta_{yzz}, \beta_{zzz}$) are utilized a frequency job output file of GAUSSIAN-09W [12]. Since the values of the mean polarizabilities (α) and mean first-order hyperpolarizability (β) of GAUSSIAN-09W output are reported in atomic units (a.u.), the calculated values have been converted into electrostatic units (esu) (α: 1 a.u. = 0.1482 × 10^{-24} esu; β:1 a.u. = 8.6393 × 10^{-33} esu) [22].

3. Results and Discussion

3.1. Molecular geometry

The crystal structure of oxamyl, $C_7H_{13}N_3O_3S$ [systematic name: (Z)-methyl 2-dimethyl-amino-N-(methylcarbamoyloxy)-2-oxoethanimidothioate], was obtained from the Cambridge Crystallographic Data Center (CCDC 1516996). The studied molecule belongs to the orthorhombic system and the space group is *Pca2₁*. The crystal structure parameters of the studied compound are found to be *a* = 8.3367(4) Å, *b* = 10.7752(5) Å, *c* = 24.1016(12) Å, β = 90°, and *V* = 2165.04(18) Å^3 [6]. The atom numbering scheme of the title compound is shown in Fig. 1.

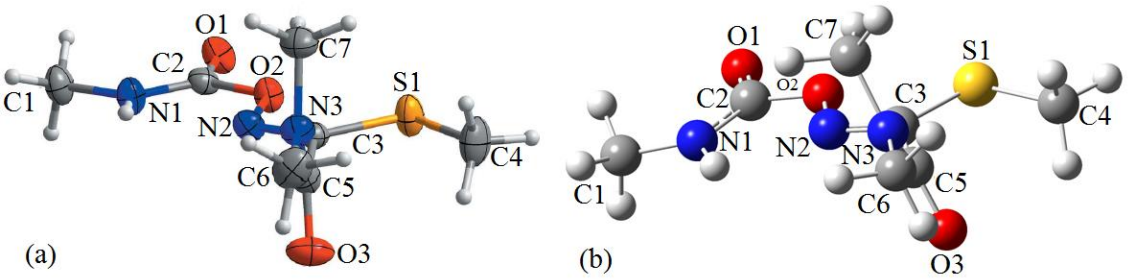

Figure 1. (a) The experimental geometric structure [6] and (b) the optimized molecular structure of oxamyl obtained from B3LYP/6-311++G(d,p) level.

The obtained theoretical results are compared with the experimental results [6] of the studied molecule and are presented in Table 1. As can be seen from Table 1, from the crystalline structure of oxamyl, the O1=C2 and O3=C5 distances were defined as 1.218(4) Å and 1.216(4) Å [6], respectively. The O1=C2 and O3=C5 distances of title compound were calculated as 1.1842 and 1.2053 Å for the HF level and 1.959 and 1.2223 Å for the DFT/B3LYP level, respectively, exhibiting partial double bond character [23, 24].

Table 1. Experimental [6] and calculated bond lengths and bond angles with HF/6-311++G(d,p) and B3LYP/6-311++G(d,p) methods of the title compound.

	Exp.	Theoretical	
Bond Lengths(Å)	X-Ray [6]	HF	B3LYP
S1–C3	1.737(3)	1.7595	1.7634
S1–C4	1.811(3)	1.8172	1.8321
O1–C2	1.218(4)	1.1842	1.2053
O2–C2	1.371(3)	1.3566	1.3965
O2–N2	1.440(3)	1.3675	1.4139
O3–C5	1.216(4)	1.1959	1.2223
N1–C2	1.323(4)	1.3392	1.3500
N1–C1	1.451(4)	1.4486	1.4544
N2–C3	1.279(4)	1.2525	1.2802
N3–C5	1.334(4)	1.3439	1.3599
N3–C7	1.455(4)	1.4536	1.4593
N3–C6	1.464(4)	1.4539	1.4598
C3-C5	1.521(4)	1.5202	1.5214
Corr. coefficient		0.9928	0.9962
Bond Angles(°)			
C3–S1–C4	102.89(1)	102.581	102.273
C2–O2–N2	114.5(2)	116.588	115.096
C2–N1–C1	120.5(2)	120.318	121.017
C3–N2–O2	108.1(2)	112.172	110.922
C5–N3–C7	124.6(3)	124.792	125.119
C5–N3–C6	118.9(3)	114.116	118.918
C7–N3–C6	116.3(3)	110.679	115.921
Corr. coefficient		0.8872	0.9885

The N1–C1, N3–C7, and N3–C6 bond lengths were found to be 1.451(4), 1.455(4), and 1.464(4) Å [6]. From Table 1, these bond lengths were calculated at 1.4486, 1.4536, and 1.4539 Å for the HF level and 1.4544, 1.4593, and 1.4598 Å for the DFT/B3LYP level. The N1–C2 and N3–C5 bond lengths for the title compound were observed to be 1.323(4) and 1.334(4) Å [6], whereas the N2-C3 bond distance was found as 1.279(4) Å [6]. Herein N1–C2 and N3–C5 bond lengths have been calculated at 1.3392 and 1.3439 Å for the HF/6-311++G(d,p) level and at 1.3500 and 1.3599 Å for B3LYP/6-311++G(d,p) level, respectively, whereas the N2-C3 bond distance was calculated as 1.2525 and 1.2802 Å using the HF and DFT/B3LYP methods, respectively. As a result of our calculations, N2–C3 bond shows typical double-bond characteristic whereas N1-C2 and N3–C5 bonds show single-bond characteristic. All of the given geometrical parameters are in good agreement with literature [25].

The bond lengths of S1–C3 and S1–C4 found to be 1.737(3)–1.811(3) Å are calculated to be 1.7595 and 1.8172 Å for the HF level and 1.7634 and 1.8321 Å for the DFT/B3LYP level, respectively.

The linear correlation coefficient (R^2) values were found to be 0.9928 and 0.9962 (for bond lengths), and 0.8872 and 0.9885 (for bond angles) for the HF and DFT/B3LYP levels, respectively (Fig. 2).

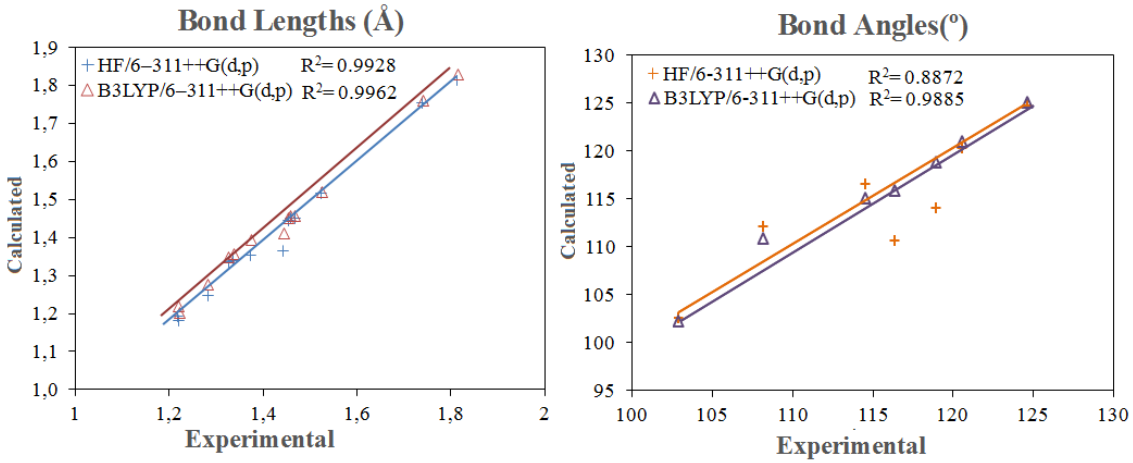

Figure 2. Linear relationships of experimental [6] and calculated (with 6-311++G(d,p) basis set) molecular bond lengths and molecular bond angles of oxamyl.

3.2. Frontier Molecular Orbitals (FMOs)

The frontier molecular orbitals (FMOs) called the highest occupied molecular orbital (HOMO) and the lowest unoccupied molecular orbital (LUMO) play a significant role in electronic, electric, and optical properties as well as in the quantum chemistry [26]. The LUMO is the lowest energy orbital that has the scope to accept electrons and hence it acts as an electron acceptor and characterizes the susceptibility of the molecule toward attack by nucleophiles. The HOMO is the outermost higher energy orbital containing electrons and hence it acts as an electron donor and characterizes the susceptibility of the molecule toward attack by electrophiles [27]. The energy difference between the LUMO and HOMO energies which is called as energy gap helps characterize the chemical reactivity and kinetic stability of the molecule. A soft molecule has the small $\Delta E_{\text{LUMO–HOMO}}$ energy gap and is more reactive and less stable than hard one with the large $\Delta E_{\text{LUMO–HOMO}}$ energy gap [28, 29]. The pictorial representations of the HOMO and LUMO of oxamyl using the DFT/B3LYP/6-311++G(d,p) calculation for gas phase are shown in Fig. 3(a) and (b).

As seen from Fig. 3(a) and (b), the positive phase is represented by the red color and the negative one is by the green color. The LUMO and HOMO are largely localized over the whole molecular moiety except for the methyl groups attached to the N atoms. Gauss-Sum 3.0 program [30] was used to prepare the density of states (DOS) spectra in Fig. 4. DOS plot demonstrates a simple view of the character of the molecular orbitals in a certain energy range and energy gap of a molecule.

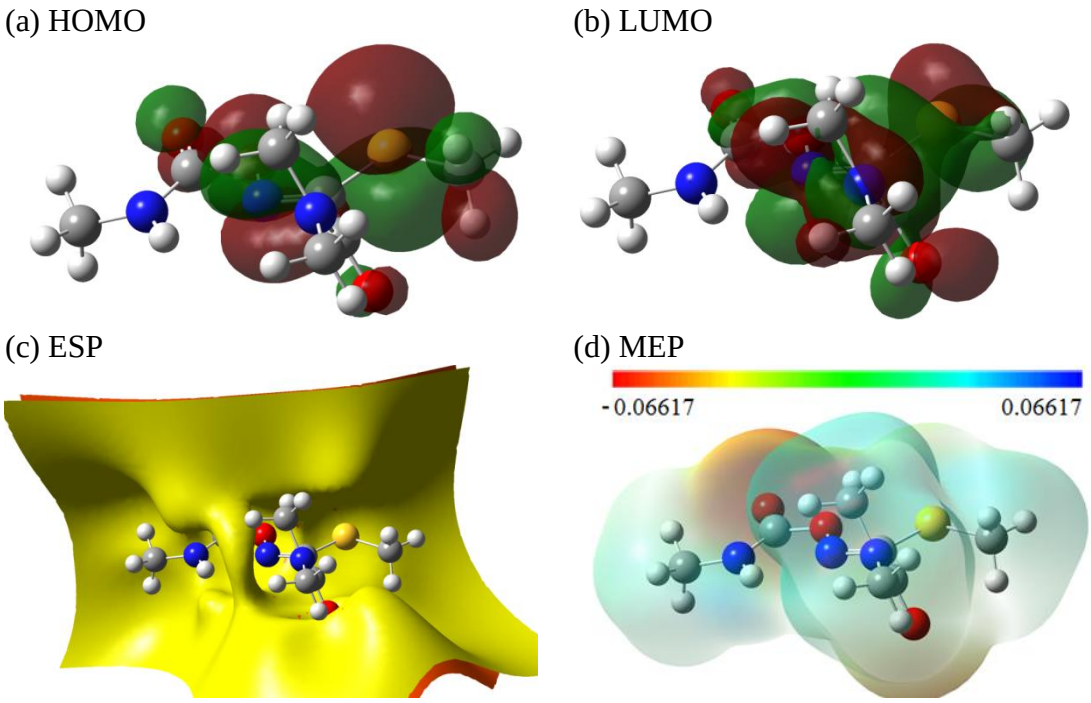

Figure 3. The 3D orbital pictures of (a) the HOMO, (b) the LUMO, (c) the electrostatic potential (ESP) and (d) the molecular electrostatic potential (MEP) by the DFT/B3LYP/6-311++G(d,p) level for oxamyl

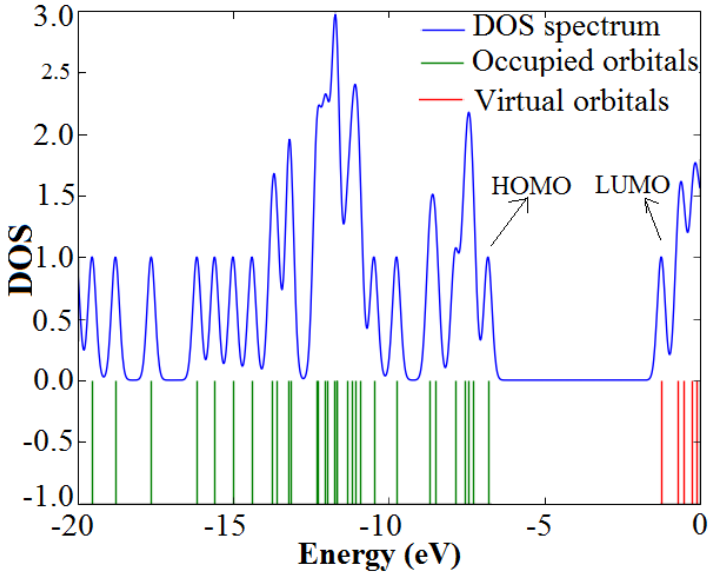

Figure 4 Density of states (DOS) diagrams for oxamyl.

The total energy, HOMO and LUMO energies, and the $\Delta E_{\text{LUMO–HOMO}}$ energy gap of the studied compound are given in Table 2. The HOMO and LUMO energies were calculated as -9.8313 and 0.7755 eV for the HF level and -6.8136 and -1.2408eV for the DFT/B3LYP level, respectively. The energy gap between the HOMO and LUMO orbitals was calculated as 10.6068 and 5.5728 eV for the HF and DFT/B3LYP levels, respectively, which clearly indicates that the molecule is quite stable. In addition, the energy gap between the HOMO and LUMO orbitals facilitates the intramolecular charge transfer that makes the material NLO active.

Table 2. Total energy (in a.u.), E_{HOMO}, E_{LUMO}, $\Delta E_{LUMO-HOMO}$, ionization potential I, electron affinity A, global hardness η, electronegativity χ, (all in eV), and global softness σ (in eV^{-1}) values of oxamyl obtained by the HF and DFT/B3LYP levels with 6-311++G(d,p) basis set.

	HF/6-311++G(d,p)	B3LYP/6-311++G(d,p)
Total Energy	-1058.2496	-1062.8818
E_{HOMO}	-9.8313	-6.8136
E_{LUMO}	0.7755	-1.2408
$\Delta E_{LUMO-HOMO}$	10.6068	5.5728
I	9.8313	6.8136
A	-0.7755	1.2408
η	5.3034	2.7864
$\sigma(eV^{-1})$	0.1886	0.3589
χ	4.5279	4.0272

3.3. Global reactivity descriptors

Development of new chemical reactivity descriptors has gained significant momentum due to their applications in various areas of chemistry, biology, rational drug design and computer-aided toxicity prediction [31]. Global hardness (η), global softness (σ), and electronegativity (χ) are global reactivity descriptors, highly successful in predicting global chemical reactivity trends.

Associated within the framework of Self-Consistency Function (SCF) Molecular Orbital (MO) theory, the ionization potential (I) and electron affinity (A) can be expressed through E_{HOMO} and E_{LUMO} orbital energies as $I = -E_{HOMO}$ and $A = - E_{LUMO}$. The obtained values of I and A were considered with most popularly used formulas for the computation of global hardness, global softness and electronegativity. Various reactivity descriptors as global hardness (η), global softness (σ) and electronegativity (χ) were evaluated using the standard working Eqs. (1-4) and these values calculated with the HF/6-311++G(d,p) and DFT/B3LYP/6-311++G(d,p) levels were listed in Table 2. The global hardness (η) and global softness (σ) correspond to the gap between the E_{HOMO} and E_{LUMO} orbital energies and have been associated with the stability of chemical system. A soft molecule has a small energy gap and is more reactive than hard one because it could easily offer electrons to an acceptor. The values of η and σ of the title molecule are 5.3034 eV (0.1886 eV^{-1}) and 2.7864 eV (0.3589 eV^{-1}) for the HF and DFT/B3LYP levels, respectively. As can be seen from Table 2, the global hardness values of title molecule are high. Hence, we conclude that the title compound belongs to a hard material.

3.4. Molecular electrostatic potential (MEP) and electrostatic potential (ESP) analyses

Molecular electrostatic potential (MEP), $V(r)$, at a given point $r(x, y, z)$ in the vicinity of a molecule, is defined in terms of the interaction energy between the electrical charge generated from the molecule's electrons and nuclei and a positive test charge (a proton) located at r. For the system studied the $V(r)$ values were calculated as described previously using the equation 10 , where Z_A is the charge of nucleus A, located at R_A, $\rho(r')$ s the electronic density function of the molecule, and r' is the dummy integration variable [32].

$$V(r) = \sum_A \frac{Z_A}{(R_A - r)} - \int \frac{\rho(r')}{(r' - r)} dr' \quad (10)$$

In the present study, the 3D plots of electrostatic potential (ESP), and molecular electrostatic potential (MEP) of oxamyl at B3LYP/6-311++G(d,p) level are illustrated in Fig. 3(c) and (d). The color scheme for the MEP surface is red, electron rich, partially negative charge; blue, electron deficient, partially positive charge; light blue, slightly electron deficient region; yellow, slightly electron rich region; and green, neutral. The color code for the maps is in the range between -0.06617 a.u. (deepest red) and 0.06617 a.u. (deepest blue) of title molecule. The MEP map of title molecule is shown in Fig. 3(d), whereas electrophilic attack is presented by negative (red) regions, nucleophilic reactivity is shown by positive (blue) regions. As seen from the Fig. 3(d), the red regions are mainly localized on the C=O, showing most favorable site for electrophilic attack. On the other hand, when focused on positive regions of the electrostatic potential, we found that the methyl groups are surrounded by blue color, indicating that these sites are probably involved in nucleophillic processes. It can be seen from the ESP figure (Fig. 3(c)), that the negative ESP is localized more over the C=O and is reflected as a yellowish blob and the positive ESP is localized on the rest of the molecules.

3.5. NonLinear optic (NLO) properties

In order to investigate the relationship among molecular structure and nonlinear optic properties (NLO), the dipole moments (μ), the mean polarizabilities (α), the anisotropy of the polarizabilities ($<\Delta\alpha>$) and the mean first-order hyperpolarizabilities (β) for oxamyl were calculated using the HF/6-311++G(d,p) and B3LYP/6-311++G(d,p) levels, based on the finite-field approach and were summarized in Table 3. The dipole moment (μ) in a molecule is an important property, which is mainly used to study the intermolecular interactions involving the non-bonded type dipole–dipole interactions, because the higher the dipole moment, the stronger the intermolecular interactions will be [33]. As can be seen from Table 3, the predicted results at different levels of computations do not differ much. The permanent dipole moment was found to be 3.1672 D for the HF level and 2.9575 D for the DFT/B3LYP level, almost independent of the basis set, and the stronger dipole moments in the case of the studied compound are primarily attributed to an overall imbalance in the charge from one side of a molecule to the other side. As shown in Table 3, the calculated polarizabilities have nonzero values and are dominated by the diagonal components. The calculated polarizability values are equal to 17.82×10^{-24} esu for the HF level and 19.92×10^{-24} esu for the DFT/B3LYP level with the 6-311++G(d,p) basis set. It is observed that the polarizability value calculated at the HF level was close to ~120 a.u., but with the same basis set for the DFT/B3LYP level, it was ~14% higher in comparison to other applied method. In this study, the mean first-order hyperpolarizabilities (β) were calculated at 0.67×10^{-30} and 1.49×10^{-30} esu using the HF and DFT/B3LYP levels, respectively. The energy gap between the HOMO and LUMO orbitals of the title compound is 10.6068 eV and 5.5728 eV for the HF and B3LYP levels, respectively. As expected, the high values of β correspond to the low HOMO–LUMO gap [34]. Urea is one of the prototypical molecules used for studying the NLO properties of the molecular systems. Therefore, it is frequently used as a threshold value for comparative purposes. The value of β for oxamyl was highly increased from 0.67×10^{-30} esu for the HF level to 1.49×10^{-30} esu for the DFT/B3LYP method with the same basis set. The β values obtained from the HF and DFT/B3LYP levels are approximately 3 and 8 times greater

than the magnitude of urea (for urea β is found to be 0.1947×10^{-30} esu), respectively. The large value of β calculated by the HF and DFT/B3LYP methods shows that the title compound is an attractive molecule for future studies of NLO properties. Consequently, from the above discussion on the contents of Table 3, we can finally deduce that the introduction of electron correlation using the method applied for the analysis of the hyperpolarizability, such as the DFT method that is based on the Kohn–Sham equations, will probably predict results better than those obtained by using the HF method that yields very poor results.

Table 3. Dipole moment μ (D), the mean polarizability $<\alpha>$ (in a.u. and esu), the anisotropic of the polarizability $\langle\Delta\alpha\rangle$ (in a.u.) and the mean first-order hyperpolarizability (β) (in a.u. and esu) values obtained using the HF/6-311++G(d,p) and B3LYP/6-311++G(d,p) methods for oxamyl.

	HF/6-311++G(d,p)	B3LYP/6-311++G(d,p)
μ (D)	3.1672	2.9575
$<\alpha>$ (a.u.)	120.25	134.39
$<\alpha> \times 10^{-24}$ (esu)	17.82	19.92
$\langle\Delta\alpha\rangle$ (a.u.)	48.43	58.78
β (a.u)	77.13	172.45
$\beta_{tot} \times 10^{-30}$ (esu)	0.67	1.49
β_{tot}/β_{urea}	3.44	7.65

3.6. Vibrational (FT-IR) analysis

The experimental vibrational spectra of oxamyl have been obtained by Hernández et. al. [1]. However, any theoretical data of this compound for vibrational analyses have not given in literature. Therefore, unscaled and scaled theoretical frequencies using DFT/B3LYP level of theory with 6-311++G(d,p) basis set along with their IR intensities, probable assignments and potential energy distribution (PED) performed by means of VEDA 4 program [11] of oxamyl are presented in Table 4 in comparison with the experimental [1] results. The scale factors are used to obtain the best agreement results between the calculated and experimental frequencies. The vibrational frequencies of the title compound are calculated with these methods and then wavenumbers in the ranges from 4000 to 1700 cm^{-1} and lower than 1700 cm^{-1} are scaled with 0.958 and 0.9067, and 0.983 and 0.908 in the DFT/B3LYP and HF levels, respectively [35]. For a visual comparison, the observed and simulated FT-IR spectra for oxamyl in HF/6-311++G(d,p) and B3LYP/6-311++G(d,p) methods are shown in Fig. 5. As seen Fig. 5, the experimental fundamentals are in better agreement with the scaled fundamentals.

3.6.1. Methyl group vibrations

The stretching vibrations of methyl (CH_3) group possess the asymmetric and symmetric stretches are expected in the range 2905-3000 cm^{-1} and 2860-2870 cm^{-1}, respectively [36]. Moreover, the asymmetric stretch is usually at higher frequencies than the symmetric stretch. The first of these result from asymmetric stretching $\nu_{as}(CH_3)$ modes in which two C-H bonds of the methyl group are extending while the third one is contracting and the other result from symmetric stretching $\nu(CH_3)$ in which all three of the C-H bonds extend and contract in-phase. The FT-IR bands observed at 3019 and 2932 cm^{-1} are assigned to the methyl group stretching vibration [37]. The HF/6-

311++G(d,p) and B3LYP/6-311++G(d,p) calculations give bands in the range 3015-2920 cm^{-1} and 3026-2938 cm^{-1} as the asymmetric stretching modes of methyl group, respectively, whereas the CH_3 symmetric modes are found at 2928 and 2891 cm^{-1} using B3LYP/6-311++G(d,p) level and at 2903 and 2872 cm^{-1} using HF/6-311++G(d,p) level. These peaks are quite pure modes with the 86–100% contribution of PED. As would be expected, asymmetric vibrations are calculated at higher wavenumbers than symmetric ones. The methyl in-plane bending vibrations have been observed at 1507 and 1386 cm^{-1} in the FT-IR spectra. The calculated vibrations, which fall in the region 1514 and 974 cm^{-1} for the HF level and 1512–967 cm^{-1} for the DFT/B3LYP level are assigned to the in-plane bending vibrations of the methyl group, these modes are contributed to the range 11–95%.

3.6.2. C=O and C-O vibrations

The structural unit of carbonyl (C=O) has an excellent group frequency which is described as a stretching vibration, and this group has been most extensively studied by infrared spectroscopy. The appearance of a strong band in IR spectra around 1650–1800 cm^{-1} shows the presence of carbonyl group and is due to the ν(C=O) stretching motion [38]. The double bond between the carbon–oxygen atoms is formed by π-π bonding between carbon and oxygen. Because these atoms have different electronegativities, the bonding electrons are not equally distributed between the two atoms. The title compound shows the sharp intense absorption bands in the 1717 cm^{-1} due to the both carbonyl (C=O) groups of oxamyl. The calculated absorptions at 1783 (78%), 1719 (81%) cm^{-1} and 1748 (78%), 1685 (81%) cm^{-1} using the HF/6-311++G(d,p) and B3LYP/6-311++G(d,p) methods, respectively, are modes 14 and 15 which belongs to the stretching of bond C=O of oxamyl. The theoretically C–O stretching bands were calculated at 1118, 1085, and 568 cm^{-1} for the HF level and at 1094, 934, and 553 cm^{-1} for the DFT/B3LYP level. The C–O in-plane and out-of- plane bending vibrations have also been identified and are listed in Table 4.

3.6.3. C=N, C-N, and C-S vibrations

The identification of the C=N and C-N stretching wavenumbers in the side chains is a difficult task, since there are problems in distinguishing these wavenumbers from other vibrations. The characteristic region of 1700–1500 cm^{-1} can be used to identify the proton transfer of C=N group. The peak experimentally observed at 1664 cm^{-1} [1] was calculated at 1701 and 1602 cm^{-1} for the HF and DFT/B3LYP levels with 90% contribution of PED, respectively. In the present work, the calculated frequencies for the ν(C-N) vibrations were obtained in the range of 1420–623 cm^{-1} and 1403–610 cm^{-1} using the HF and DFT/B3LYP methods, respectively, and show excellent agreement with the literature [39]. As indicated by PED, these modes are contributed to the range 10–42%. The C-S group has a considerably weaker band. In consequence, the bond is not intense, and it falls at lower frequencies. Identification is therefore difficult and uncertain [40]. In this study, the theoretically scaled vibrations by HF/6-311++G(d,p) and DFT/B3LYP/6-311++G(d,p) methods at 708, 695, 681, and 568 cm^{-1} and 696, 686, 676, and 553 cm^{-1}, respectively, are assigned to ν(SC) stretching vibrations. These band values calculated at the same methods are in good agreement with the corresponding band values; 745 and 732, respectively [34].

3.6.4. N-H vibrations

A non-hydrogen-bonded or a free hydroxyl group gives peaks at the range of 3550–3700 cm^{-1} [41]. In this present study, the N-H stretching vibration (see Fig. 5) which is

a pure mode with the 100% contribution of PED was calculated as 3549 and 3470 cm^{-1} of title compound by using the HF and DFT/B3LYP methods with 6-311++G(d,p) basis set, respectively. This stretching has been observed at 3335 cm^{-1} [1]. As seen from PED analysis in Table 4, the N-H in-plane bending vibrations contribute to the calculated four frequencies at 1539, 1256, and 1183 cm^{-1} (HF level) and 1524, 1218, and 1170 cm^{-1} (DFT/B3LYP level). These frequencies were assigned to the bands at 1570 and 1243 cm^{-1} in the FT-IR. As evidenced from PED contributions in Table 4, these modes are contributed to the range 12–44%. The scaled vibrational frequencies computed by HF/6-311++G(d,p) and DFT/B3LYP/6-311++G(d,p) methods at 436 and 524 cm^{-1} with PED contribution of 89%, respectively, were assigned to the N-H out-of-bending (γHNCO) vibration.

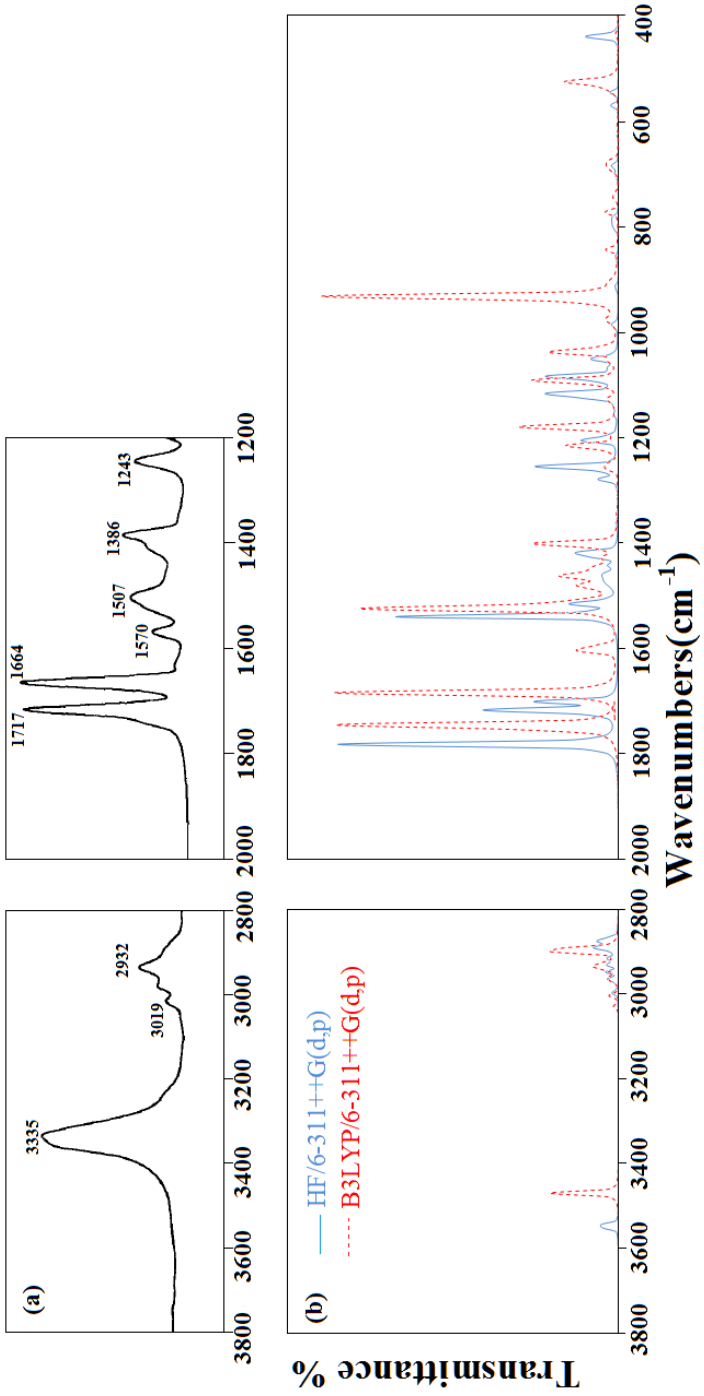

Figure 5. (a) The experimental [1] and (b) the simulated FT-IR spectrum computed at HF and DFT/B3LYP levels with 6-311++G(d,p) basis set of oxamyl.

Table 4 Comparison of the observed (FT-IR) and calculated vibration frequencies (ν, cm^{-1}), IR intensities (I_{IR}, km/mol) and potential energy distribution (PED) using the HF/6-311++G(d,p) and B3LYP/6-311++G(d,p) of oxamyl.

		Exp.	Theoretical							
		FT-IR	HF/6-311++G(d,p)				B3LYP/6-311++G(d,p)			
ν	Assignments (%PED[a])		A[b]	B[c]	IR Int.	R. Act.	A[b]	B[c]	IR Int.	R. Act.
1	ν(NH) (100)	3335	3914	3549	98	47	3622	3470	90	79
2	$\nu_{as}(CH_3)$ (87)	3019	3325	3015	2	34	3159	3026	0	39
3	$\nu_{as}(CH_3)$ (97)		3314	3005	2	44	3163	3030	1	44
4	$\nu_{as}(CH_3)$ (86)		3306	2998	16	32	3162	3029	6	25
5	$\nu_{as}(CH_3)$ (100)		3283	2977	10	73	3137	3005	6	76
6	$\nu_{as}(CH_3)$ (100)		3271	2966	26	64	3134	3002	7	56
7	$\nu_{as}(CH_3)$ (100)		3253	2950	30	66	3095	2965	23	92
8	$\nu_{as}(CH_3)$ (99)	2932	3233	2931	34	85	3070	2941	1	21
9	$\nu_{as}(CH_3)$ (100)		3220	2920	35	71	3067	2938	48	169
10	$\nu(CH_3)$ (100)		3202	2903	21	152	3056	2928	16	182
11	$\nu(CH_3)$ (99)		3189	2891	61	161	3026	2899	63	241
12	$\nu(CH_3)$ (92)		3176	2880	70	235	3023	2896	80	346
13	$\nu(CH_3)$ (93)		3167	2872	38	52	3018	2891	21	28
14	ν(C=O) (78)	1717	1966	1783	732	13	1825	1748	524	37
15	ν(C=O) (81)		1896	1719	392	37	1715	1685	381	14
16	ν(C=N) (90)	1664	1877	1701	229	59	1630	1602	93	65
17	σ(HNC) (44), σ(HCH) (16), ν(C=N) (13)	1570	1695	1539	599	5	1550	1524	402	15
18	σ(HCH) (58)	1507	1667	1514	146	8	1538	1512	60	7
19	σ(HCH) (59)		1635	1485	16	6	1510	1484	60	5
20	σ(HCH) (63), τ(HCNC) (12)		1624	1475	21	3	1504	1478	11	4
21	σ(HCH) (63)		1614	1466	28	10	1498	1473	13	3
22	σ(HCH) (58)		1608	1460	15	6	1488	1463	4	7
23	σ(HCH) (49)		1602	1455	10	11	1474	1449	22	17
24	τ(HCSC) (17), σ(HCH) (71)		1590	1444	10	10	1467	1442	18	11
25	σ(HCH) (83)		1588	1442	11	3	1454	1429	15	5
26	σ(HCH) (67)		1568	1424	33	6	1437	1413	11	5
27	ν(CN) (34)		1564	1420	162	1	1427	1403	115	24
28	σ(HCH) (95)	1386	1497	1359	6	0	1367	1344	3	2
29	ν(CN) (42), σ(CNC) (11)		1408	1279	47	1	1278	1256	35	1
30	δ(HNC) (12), ν(CN) (14)	1243	1383	1256	260	2	1239	1218	86	5
31	ν(CC) (13), ν(CN) (27)		1324	1202	138	3	1202	1182	130	7
32	σ(HNC) (12), δ(HCH) (11), τ(HCNC) (32)		1303	1183	2	4	1190	1170	3	4
33	τ(HCNC) (54)		1270	1153	10	1	1169	1149	3	0
34	δ(HCH) (17), τ(HCNC) (66)		1256	1140	1	2	1150	1131	21	3
35	ν(OC) (20), ν(CN) (39),		1231	1118	312	4	1113	1094	139	4
36	ν(CN) (21)		1154	1048	85	6	1055	1037	121	6
37	δ(HCH) (11), τ(HCSC) (63)		1086	986	23	2	997	980	20	2
38	τ(HCSC) (66), δ(HCH) (10)		1073	974	2	1	984	967	4	2
39	ν(OC) (23), ν(ON) (55)		1195	1085	263	3	950	934	442	6
40	ν(CN) (33)		1007	914	15	10	919	903	9	8
41	ν(ON) (11), ν(CN) (17)		944	857	13	2	859	844	16	4
42	σ(CON) (10), σ(CCN) (11), γ(ONCC) (42)		881	800	24	2	787	774	17	2
43	γ(ONOC) (86)		864	785	34	1	756	743	13	1
44	ν(SC) (33), σ(OCO) (12), γ(ONCC) (13)		780	708	3	7	708	696	9	7
45	ν(CN) (10), ν(SC) (30), σ(NCC) (15)		765	695	16	8	698	686	13	3
46	ν(SC) (37), σ(NCC) (11)		750	681	18	12	688	676	12	10
47	γ(SCNC) (26), ν(CN) (20), σ(OCC) (29)		686	623	5	4	621	610	3	2
48	ν(OC) (14), ν(SC) (27)		626	568	21	1	563	553	1	1
49	σ(OCO) (28), σ(NCO) (18), σ(CON) (10)		598	543	22	2	547	537	31	4
50	τ(HNCO) (89)		480	436	86	1	533	524	78	1

4. Conclusions

In the present study, the detailed investigations on oxamyl were performed using quantum chemical calculations. The structural, electronic, and vibrational frequencies of the title compound have been calculated by the HF/6-311++G(d,p) and

DFT/B3LYP/6-311++G(d,p) methods. The optimized geometric parameters (bond lengths and bond angles) of oxamyl are theoretically determined and compared with the experimental results. On the basis of the agreement between the calculated and observed results, assignments of fundamental vibrational modes of the title compound were examined based on the results of the PED output obtained from normal coordinate analysis. After scaling down, the calculated wavenumbers show good agreement with the FT-IR spectra. The nonlinear optical property of the studied compound was investigated by determining the ground-state dipole moment, the mean polarizability, the anisotropy of the polarizability, and the mean first-order hyperpolarizability using the HF and DFT/B3LYP levels with 6-311++G(d,p) basis set. Finally, it is demonstrated that the investigated compound can be used as a NLO material. Besides, the global reactivity descriptors have been calculated and discussed.

References

[1] García Hernández J.E., Notario del Pino J.S., González Martín M.M., Díaz Díaz R. and Febles González E.J., Natural phillipsite as a matrix for a slow-release formulation of oxamyl, **Environmental Pollution**, 88, 355-359, (1995).

[2] Worthing C.R. and Hance R.J., **The Pesticide Manual**, 637, 9th Edn. British Crop Protection Council, (1991).

[3] Leistra M., **Behaviour and significance of pesticide residues in ground water,** Aspects of Applied Biology, 17, 223-229, (1988).

[4] Ecobicon D.J., **Toxic effects of pesticides**, in Klassen, C.D., (Ed.), Casarett & Doull's Toxicology, *The Basic Science of Poisons*, 763-810, McGraw-Hill, New York, (2001).

[5] United States Environmental Protection Agency (USEPA), Carbamate cumulative assessment group for the N-methyl carbamates, (2004). http://www.epa.gov.

[6] Kwon E., Park K., Park H. and Kim T., Crystal structure of oxamyl, **Acta Crystallographica**, E72, 1816–1818, (2016).

[7] Frisch M.J., Trucks G.W., Schlegel H.B., Scuseria G.E., Robb M.A., Cheeseman J.R., Scalmani G., Barone V., Mennucci B., Petersson G.A., Nakatsuji H., Caricato M., Li X., Hratchian H.P., Izmaylov A.F., Bloino J., Zheng G., Sonnenberg J.L., Hada M., Ehara M., Toyota K., Fukuda R., Hasegawa J., Ishida M., Nakajima T., Honda Y., Kitao O., Nakai H., Vreven T., Montgomery Jr. J.A., , Peralta J.E., Ogliaro F., Bearpark M., Heyd J.J., Brothers E., Kudin K.N., Staroverov V.N., Kobayashi R., Normand J., Raghavachari K., Rendell A., Burant J.C., Iyengar S.S., Tomasi J., Cossi M., Rega N., Millam J.M., Klene M., Knox J.E., Cross J.B., Bakken V., Adamo C., Jaramillo J., Gomperts R., Stratmann R.E., Yazyev O., Austin A.J., Cammi R., Pomelli C., Ochterski J.W., Martin R.L., Morokuma K., Zakrzewski V.G., Voth G.A., Salvador P., Dannenberg J.J., Dapprich S., Daniels A.D., Farkas Ö., Foresman J.B., Ortiz J. V., Cioslowski J. and Fox D. J., **Gaussian 09, Revision A.11.4,** Gaussian Inc., Wallingford CT, (2009).

[8] Dennington R., Keith T. and Millam J., **GaussView, Version 5.0.9**, Semichem Inc., Shawnee Mission, KS, (2009).

[9] Becke A.D., Density-functional thermochemistry. III. The role of exact exchange, **Journal of Chemical Physics**, 98, 5648-5652, (1993).

[10] Lee C.T., Yang W.T. and Parr R.G., Development of the Colle-Salvetti correlation-energy Formula into a functional of the electron density, **Physical Review B**, 37, 785-789, (1988).

[11] Jamróz M.H. and Dobrowolski J. Cz., Potential Energy Distribution Analysis (PED) of DFT Calculated IR Spectra of the most Stable Li, Na, Cu(I) Diformate Molecules, **Journal of Molecular Structure**, 565–566, 475–480, (2001).

[12] Sivaranjani T., Periandy S. and Xavier S., Conformational stability, molecular structure, vibrational, electronic, 1H and 13C spectral analysis of 3-pyridinemethanol using ab-initio/DFT method, **Journal of Molecular Structure**, 1108, 398-410, (2016).

[13] Koopmans T.C., About the allocation of wave functions and eigenvalues of the individual electrons one atom, **Physica (Amsterdam)**, 1, 104-112, (1934).

[14] Senet P., Chemical hardnesses of atoms and molecules from frontier orbitals, **Chemical Physics Letters**, 275, 527-532, (1997).

[15] Pauling L., **The Nature of the Chemical Bond**, Cornell University Press, Ithaca, New York, (1960).

[16] Hinchliffe A., Nikolaidi B. and Machado H.J.S., Density Functional Studies of the Dipole Polarizabilities of Substituted Stilbene, Azoarene and Related Push-Pull Molecules, **International Journal of Molecular Sciences**, 5(8), 224-238, (2004).

[17] Buckingham A.D., Permanent and Induced Molecular Moments and Long-Range Intermolecular Forces, **Advances in Chemical Physics**, 12, 107-142, (1967).

[18] Mclean A.D. and Yoshimine M., Theory of Molecular Polarizabillities, **The Journal of Chemical Physics**, 47, 1927, (1967).

[19] Lin C. and Wu K., Theoretical studies on the nonlinear optical susceptibilities of 3-methoxy-4-hydroxy-benzaldehyde crystal, **Chemical Physics Letters**, 321, 83-88, (2000).

[20] Abraham J.P., Sajan D., Hubert I.J. and Jayakumar V.S., Molecular structure, spectroscopic studies and first-order molecular hyperpolarizabilities of p-amino acetanilide, **Spectrochimica Acta Part A: Molecular and Biomolecular Spectroscopy**, 71, 355-367, (2008).

[21] Karamanis P., Pouchan C. and Maroulis G., Structure, stability, dipole polarizability and differential polarizability in small gallium arsenide clusters from all-electron ab initio and density-functional-theory calculations, **Physical Review A**, 77, 013201-013203, (2008).

[22] Eşme A., Sağdınç S.G., Theoretical Studies of Molecular Structures, Infrared Spectra, NBO and NLO Properties of Some Novel 5-arylazo-6-hydroxy-4-phenyl-3-cyano-2-pyridone Dyes, Acta Physica Polonica A, 130, 1273-1287, (2016).

[23] Huang W., and Qian H., Structural characterization of C.I. Disperse Yellow 114", **Dyes and Pigments**, 77, 446-450, (2008).

[24] Raja M., Raj Muhamed R., Muthu S. and Suresh M., Synthesis, spectroscopic (FT-IR, FT-Raman, NMR, UV-Visible), NLO, NBO, HOMO-LUMO, Fukui function and molecular docking study of (E)-1-(5-bromo-2-hydroxybenzylidene)semicarbazide, **Journal of Molecular Structure**, 1141, 284-298, (2017).

[25] Öner N., Tamer Ö., Avcı D. and Atalay Y., Conformational, spectroscopic and nonlinear optical properties of biologically active N,N-dimethyltryptamine

molecule: A theoretical study, **Spectrochimica Acta Part A: Molecular and Biomolecular Spectroscopy**, 133, 542-549, (2014).

[26] Fleming I., **Frontier Orbitals and Organic Chemical Reactions**, Wiley, London, (1976).

[27] Karelson M., Lobanov V.S. and Katritzky A.R., Quantum-Chemical Descriptors in QSAR/QSPR Studies, **Chemical Reviews**, 96, 1027-1044, (1996).

[28] Eşme A. and Sağdınç S.G., The vibrational studies and theoretical investigation of structure, electronic and non-linear optical properties of Sudan III [1-{[4-(phenylazo) phenyl]azo}-2-naphthalenol], **Journal of Molecular Structure**, 1048, 185-195, (2013).

[29] Çiçek B., Çakır U. and Azizoglu A., The associations of macrocyclic ethers with cations in 1,4-dioxane/water mixtures; potentiometric Na+ and K+ binding measurements and computational study, **Journal of Inclusion Phenomena and Macrocyclic Chemistry**, 72, 121-125, (2012).

[30] O'Boyle N.M., Tenderholt A.L. and Langer K.M., cclib: A library for package-independent computational chemistry algorithms, **Journal of Computational Chemistry**, 29, 839–845, (2008).

[31] Chattaraj P.K., Nath S. and Maiti B., **Computational Medicinal Chemistry for Drug Discovery**, Marcel Dekker, New York, 2003.

[32] Politzer P. and Murray J., The fundamental nature and role of the electrostatic potential in atoms and molecules, **Theoretical Chemistry Accounts**, 108, 134-142, (2002).

[33] Prasad O., Sinha L. and Kumar N., Theoretical Raman and IR spectra of tegafur and comparison of molecular electrostatic potential surfaces, polarizability and hyerpolarizability of tegafur with 5-fluoro-uracil by density functional theory, **Journal of Atomic and Molecular Sciences**, 1, 201-214, (2010).

[34] Ceylan Ü., Tarı G.Ö., Gökçe H., and Ağar E., Spectroscopic (FT–IR and UV–Vis) and theoretical (HF and DFT) investigation of 2-Ethyl-N-[(5-nitrothiophene-2-yl)methylidene]aniline, **Journal of Molecular Structure**, 1110, 1-10, (2016).

[35] Sivaranjani T., Periandy S. and Xavier S., Conformational stability, molecular structure, vibrational, electronic, 1H and 13C spectral analysis of 3-pyridinemethanol using ab-initio/DFT method, **Journal of Molecular Structure,** 1108, 398-410, (2016).

[36] Colthup N.B., Daly L.H. and Wiberly S.E., **Introduction to Infrared and Raman Spectroscopy**, Academic Press, New York, 1975.

[37] Debnath D., Roy S., Li B., Lin C. and Misra T.K., Synthesis, structure and study of azo-hydrazone tautomeric equilibrium of 1,3-dimethyl-5-(arylazo)-6-amino-uracil derivatives, **Spectrochimica Acta Part A: Molecular and Biomolecular Spectroscopy**, 140, 185–197, (2015).

[38] Srivastava R. K., Narayan V., Prasad O. and Sinha L., Vibrational, Structural and Electronic properties of 6-methyl nicotinic acid by Density Functional Theory,**Journal of Chemical Pharmaceutical Research**, 4 (6) (2012) 3287-3296.

[39] Singh G., Abbas J.M., Dogra S.D., Sachdeva R., Rai B., Tripathi S.K., Prakash S., Sathe V. and Saini G.S.S., Vibrational and electronic spectroscopic studies of melatonin, **Spectrochimica Acta Part A: Molecular and Biomolecular Spectroscopy**, 118, 73–81, (2014).

[40] Tanak H., Koysal Y., Işık Ş., Yaman H. and Ahsen V., Experimental and computational approaches to the molecular structure of 3-(2-

Mercaptopyridine)phthalonitrile, **Bulletin of Korean Chemical Society**, 32, 673-680, (2011).

[41] Teimouri A., Chermahini A. N., Taban K., Dabbagh H.A., Experimental and CIS, TD-DFT, ab initio calculations of visible spectra and the vibrational frequencies of sulfonyl azide-azoic dyes, **Spectrochimica Acta Part A: Molecular and Biomolecular Spectroscopy,** 72, 369–377, (2009).